Original Research

ORTHOPEDICS

Effects of intra-articular micro-fragmented adipose tissue alone or combined with hyaluronic acid or collagen on cartilage degeneration and oxidative stress in an experimental rabbit osteoarthritis model

Alina Otilia Adam[1], Horea Rares Ciprian Benea[1], Luciana-Mădălina Gherman[2], Daniel Oltean-Dan[1], Dragoș Apostu[1], Dan Gheban[3], Maria Crișan[4]

1) Department of Orthopedics and Traumatology, Iuliu Hatieganu University of Medicine and Pharmacy, Cluj-Napoca, Romania

2) Experimental Centre, Iuliu Hatieganu University of Medicine and Pharmacy, Cluj-Napoca, Romania

3) Department of Pathological Anatomy, Iuliu Hatieganu University of Medicine and Pharmacy, Cluj-Napoca, Romania

4) Department of Histology, Iuliu Hatieganu University of Medicine and Pharmacy, Cluj-Napoca, Romania

Abstract

Background. Osteoarthritis is a prevalent, debilitating, progressive joint disease characterized by articular cartilage degradation, synovial inflammation, and subchondral bone remodeling. This study evaluated the local structural and systemic oxidative stress effects of intra-articular human-derived micro-fragmented adipose tissue (MFAT), administered alone or combined with hyaluronic acid (HA) or injectable collagen (COL), in an experimental rabbit osteoarthritis model.

Methods. Twenty-four rabbits underwent bilateral arthroscopic anterior cruciate ligament transection. Twenty-one rabbits were allocated to MFAT, MFAT+HA, or MFAT+COL treatment groups and received intra-articular treatment in one knee at weeks 8 and 10, with the contralateral knee serving as an untreated internal control. An additional pilot cohort of three rabbits (six knees) underwent arthroscopic anterior cruciate ligament transection without treatment to characterize untreated disease progression. At week 12, outcomes included macroscopic cartilage scoring, Picrosirius Red (PSR) collagen birefringence, and serum oxidative stress profiling.

Results. Macroscopically, intra-articular interventions demonstrated a trend toward reduced cartilage degeneration relative to paired untreated knees, reaching statistical significance in the MFAT+HA and MFAT+COL groups (adjusted $p = 0.047$). Additionally, treated cohorts exhibited lower macroscopic degeneration scores compared to the untreated pilot control ($p = 0.050$), with no significant structural differences observed among the treatments themselves. Histologically, the MFAT+COL group showed an increase in PSR birefringence of thin, loosely-packed fibers compared to the paired control ($p = 0.047$). Systemically, all three MFAT-based therapies significantly decreased nitric oxide (NO) production relative to controls ($p < 0.0001$). While total antioxidant response (TAR) remained comparable across groups, total oxidative status (TOS), oxidative stress index (OSI) and the systemic lipid peroxidation marker were elevated primarily in the MFAT ($p=0.024$, $p=0.023$, 0.0085) and MFAT+HA ($p=0.013$, $p=0.013$, 0.0046) cohorts.

Conclusions. In this experimental rabbit model, intra-articular micro-fragmented adipose tissue attenuated macroscopic cartilage degeneration in the presence of uncorrected mechanical joint instability. Systemic oxidative stress findings were mixed: NO was reduced across all treated groups, while TOS, OSI, and the systemic lipid peroxidation marker were elevated in MFAT and MFAT+HA relative to control, precluding a conclusion of an overall favorable systemic oxidative stress effect. The addition of injectable collagen was associated with a shift in PSR birefringence patterns and should be regarded as hypothesis-generating rather than confirmatory of extracellular matrix remodeling given the semi-quantitative nature of this method, whereas hyaluronic acid provided no additional structural benefit under the present experimental conditions.

Keywords: osteoarthritis, micro-fragmented adipose tissue, Lipogems, cartilage, rabbit model, oxidative stress

DOI: 10.15386/mpr-3010

Manuscript received: 23.07.2026
Received in revised form: 24.08.2026 6
Accepted: 08.09.2026

Address for correspondence:
Horea Rares Ciprian Benea
beneahorea@elearn.umfcluj.ro

Introduction

Osteoarthritis (OA) is a highly prevalent, chronic, and debilitating joint disorder characterized by the progressive degradation of articular cartilage, chronic synovial inflammation, and pathological subchondral bone remodeling [1]. Clinically, it presents a profound global health burden, significantly impairing mobility and diminishing patient quality of life [2]. Current standard-of-care conservative therapies, including non-steroidal anti-inflammatory drugs (NSAIDs) and intra-articular corticosteroid injections, are predominantly palliative. While these interventions may offer temporary symptomatic relief, they fail to halt or reverse the underlying structural progression of the disease, ultimately culminating in end-stage joint failure and the necessity for surgical joint arthroplasty [3].

In response to the limitations of conservative management, the therapeutic paradigm has increasingly shifted toward disease-modifying orthobiologic interventions aimed at restoring joint homeostasis, mitigating inflammation, and promoting tissue repair [4]. Adipose tissue is an attractive source for such strategies, being abundant, accessible through minimally invasive harvesting, and a potent reservoir of mesenchymal stem cells (MSCs) and supportive structural matrices [5]. Clinical and preclinical interest has focused on two principal adipose-derived products: the stromal vascular fraction (SVF) and micro-fragmented adipose tissue (MFAT) [6]. SVF isolation requires enzymatic digestion with collagenase, raising regulatory and safety concerns related to residual enzyme contamination [7]. MFAT, generated instead through purely mechanical disruption and micro-filtration, avoids these risks while preserving the intact extracellular matrix and native perivascular niche, thereby sustaining cellular viability and paracrine secretion of pro-regenerative cytokines and growth factors [8].

Because the catabolic microenvironment of an osteoarthritic joint can compromise the survival and integration of a biological graft, recent strategies have explored combining MFAT with structural adjuvants. Hyaluronic acid (HA) restores synovial viscoelasticity, joint lubrication, and mechanically shields cellular grafts from shear forces [9], whereas intra-articular collagen provides a direct biomolecular substrate for the extracellular matrix and has been shown to stimulate chondrocyte proliferation and support structural tissue repair [10]. Despite their distinct biomechanical and biological rationales, the combined efficacy of purely mechanical, human-derived MFAT with either adjuvant remains underexplored in established preclinical models.

Furthermore, osteoarthritis is increasingly recognized not merely as a localized mechanical pathology, but as a condition intimately linked to systemic oxidative stress. The progressive degradation of articular cartilage is heavily mediated by reactive oxygen species (ROS) and lipid peroxidation, which eventually overwhelm the endogenous antioxidant defense mechanisms. Consequently, chronic localized joint inflammation often translates systemically, resulting in altered serological profiles of critical oxidative stress biomarkers [11]. While the local structural and symptomatic effects of intra-articular orthobiologics are extensively documented in the literature, the influence of these localized, adipose-derived interventions on the broader systemic oxidative stress profile remains poorly characterized.

Therefore, the aim of this in vivo study was to evaluate the structural and systemic effects of intra-articular human-derived MFAT, administered both in isolation and in combination with structural adjuvants (hyaluronic acid or injectable collagen), using an arthroscopic lapine anterior cruciate ligament transection (ACLT) model of OA. It was hypothesized that intra-articular MFAT administration would attenuate macroscopic cartilage degeneration and alter extracellular matrix remodeling. Furthermore, it was hypothesized that the addition of targeted structural adjuvants would further modulate these localized chondroprotective effects and that the effective biological stabilization of the localized joint pathology would concurrently result in a measurable reduction of systemic oxidative stress parameters.

Methods

Ethical approval

All experimental procedures were approved by the Ethics Committee of the Iuliu Haţieganu University of Medicine and Pharmacy, Cluj-Napoca, Romania (Approval No. 307/13.12.2022), and by the Romanian National Sanitary Veterinary and Food Safety Authority (Approval No. 347/20.01.2023).

Human adipose tissue used for MFAT preparation was obtained from surgical waste collected during elective joint arthroplasty after written informed consent from all donors. Tissue collection and processing complied with the Declaration of Helsinki.

Animals

Twenty-four skeletally mature New Zealand White rabbits (Oryctolagus cuniculus), weighing 3.0–4.0 kg, were included in this experimental study. Animals were housed individually under controlled environmental conditions (20–22°C, 12-hour light/dark cycle) with free access to food and water. A one-week acclimatization period was allowed before any experimental procedures.

Bilateral arthroscopic ACLT was performed in all animals to induce post-traumatic OA. Twenty-one rabbits were subsequently randomly allocated to three treatment groups (n = 7 per group): MFAT, MFAT+HA, and MFAT+COL. One rabbit in the MFAT group died following ACLT before receiving treatment because of postoperative complications and was not replaced.

Consequently, six treated knees were available for analysis in the MFAT group. The selection of the intervention joint was standardized across all subjects; the left knee of each rabbit received the allocated intra-articular treatment, whereas the right knee served as the internal untreated control.

Eight weeks and ten weeks after ACLT, each rabbit from the treatment groups received the unilateral allocated intra-articular treatment.

An additional pilot control cohort consisted of three rabbits (six knees) that underwent bilateral ACLT without receiving any intra-articular treatment. These animals were used exclusively to characterize the natural progression of the experimental model.

Anesthesia and arthroscopic osteoarthritis induction

General anesthesia was induced with intramuscular ketamine (35 mg/kg) and xylazine (5 mg/kg). Both knees were aseptically prepared following local hair removal. With the animals secured in dorsal recumbency and the knees partially flexed, a single experienced orthopedic surgeon conducted the bilateral arthroscopic procedures.

Arthroscopy was performed using a 2.4-mm, 30° viewing angle arthroscope (Karl Storz, Germany). An anterolateral viewing portal was utilized for arthroscope insertion, accompanied by an anteromedial portal for surgical instrumentation. The joint space was distended with sterile isotonic saline. After diagnostic arthroscopic inspection confirmed normal intra-articular anatomy, the anterior cruciate ligament (ACL) was isolated within the intercondylar notch and completely transected using a 2.5-mm motorized shaver (Karl Storz, Germany). Successful destabilization was confirmed visually and via a positive anterior drawer test in both knees.

Portal incisions were routinely closed. A single prophylactic dose of enrofloxacin (5 mg/kg) and post-operative analgesic meloxicam (1 mg/kg) was administered. Animals resumed unrestricted weight-bearing within 48 hours without postoperative infection.

Postoperative exercise protocol

One week after ACLT, all rabbits started a standardized exercise protocol consisting of one 10-minute session of unrestricted hopping per week in an open enclosure. Animals were gently encouraged to maintain continuous locomotion throughout each session until euthanasia.

Preparation and administration of intra-articular treatments

Therapeutic interventions were administered to the designated treatment joints at 8 weeks and 10 weeks following the initial arthroscopic ACLT surgery.

MFAT was processed at the time of each injection using the Lipogems® system (Lipogems International, Milan, Italy) from discarded human surgical adipose tissue. Human MFAT was selected to reproduce the clinical product currently used in orthopedic practice and to evaluate its biological effects in a translational experimental model.

Fresh MFAT was prepared immediately before each administration. Because freshly processed tissue was required, independent donors undergoing elective arthroplasty were used at each treatment session. This approach also reflects the biological variability encountered in clinical practice.

MFAT was prepared using the Lipogems® system (Lipogems International, Milan, Italy) according to the manufacturer's instructions. The system mechanically processes lipoaspirate in a closed, enzyme-free environment through sequential washing, filtration, and mild mechanical fragmentation, generating purified injectable microfragmented adipose tissue while preserving the stromal vascular niche.

The structural adjuvants utilized for the combination groups were Proyal 80 (80 mg/4 mL; high molecular weight 2.5–3.5 MDa, non-cross-linked hyaluronic acid) (The wave innovation group, Italy) and injectable collagen Guna MD-KNEE (type I tropocollagen, 300kDA, 2x10^14 molecules of tropocollagen/2ml) (Guna, Milan, Italy).

Under sterile conditions, the selected knee of each rabbit in the intervention cohorts received the designated therapeutic protocol, while the contralateral knee remained an internal control. Combination protocols followed the manufacturers' recommended clinical administration schedules. Consequently, HA was administered only at week 8, whereas collagen was administered at both treatment sessions. Injection volumes were selected according to the joint capacity of the rabbit knee while maintaining the recommended proportions for each product (Table I).

Experimental timeline and study groups

The complete timeline for disease induction, therapeutic intervention, and evaluation are detailed in table II.

Table I. Therapeutic formulations and dosing schedule by treatment group.

Group	Week 8	Week 10
MFAT	300 µL MFAT	300 µL MFAT
MFAT+HA	300 µL MFAT + 200 µL HA	300 µL MFAT
MFAT+COL	300 µL MFAT + 200 µL COL	300 µL MFAT + 200 µL COL

Table II. Experimental timeline of arthroscopic induction, therapeutic intervention and evaluation.

Timepoint	Event	Details
Week 0	Bilateral arthroscopic ACLT	Surgical induction of joint instability
Week 1–12	Continuous mechanical loading	Weekly supervised exercise protocol to maintain standardized mechanical loading
Week 8	First treatment administration	Intra-articular injection (MFAT ± Adjuvants)
Week 10	Second treatment administration	Intra-articular injection (MFAT ± Adjuvants)
Week 12	Euthanasia and endpoint evaluation	Tissue harvesting for macroscopic, histological, biochemical, and systemic analysis

ACLT = anterior cruciate ligament transection, MFAT=micro-fragmented adipose tissue.

Sacrifice and tissue harvesting

At week 12, peripheral blood samples were collected from the marginal ear vein and centrifuged to obtain serum, which was stored at −20°C until analysis. Animals were subsequently euthanized by anesthetic overdose. After macroscopic evaluation, femoral condyles and tibial plateaus were harvested and fixed in 10% neutral-buffered formalin for histological processing.

Macroscopic evaluation

Following arthrotomy, the articular surfaces of the femoral condyles and tibial plateaus underwent gross visual inspection. The severity of macroscopic cartilage degradation was evaluated independently by two independent blinded observers utilizing the Modified Outerbridge classification system [12]. Observers were blinded to treatment allocation. This framework scores cartilage integrity on a 0 to 4 scale, where 0 indicates macroscopically intact tissue and 4 denotes full-thickness cartilage loss with exposed subchondral bone. Any inter-observer scoring discrepancies were resolved after joint review through collaborative re-evaluation to achieve a final consensus.

Histological preparation and morphometric analysis

Formalin-fixed osteochondral blocks were decalcified for 12 hours using a hydrochloric and formic acid solution (Biodec-R; Bio-Optica, Milan, Italy). Following decalcification, the specimens were rinsed in phosphate-buffered saline (pH 7.4), dehydrated, embedded in paraffin wax, and cut into 5-µm sagittal sections. Image analysis was performed using identical threshold settings for all specimens. Observers were blinded to treatment allocation.

To evaluate the extracellular matrix collagen organization, sections were stained with Picrosirius Red (PSR) and examined under polarized light microscopy [13,14]. Digital analysis of the resulting birefringence patterns was conducted using Adobe Photoshop software. Rather than identifying exact molecular collagen subtypes, this semi-quantitative technique was utilized to gauge overall matrix maturity based on fiber thickness and spatial packing. Micrographs were captured from the regions displaying the most profound pathological alterations. Orange-red birefringence was interpreted as representing predominantly thick, mature collagen fibers, whereas green birefringence represented thinner, less organized fibers, consistent with the conventional interpretation of type I- and type III-predominant collagen respectively architecture. The proportional area of each fiber architecture was then calculated by dividing the specific color pixel count by the total pixel count of the region of interest (ROI), expressing the result as a percentage. This analytical sequence was replicated to quantify both type I and type III collagen fractions.

Serum oxidative stress profiling

Systemic oxidative stress and antioxidant capacity were evaluated from the collected serum samples according to previously published methods [15]. Total oxidative status (TOS) and total antioxidant response (TAR) were quantified and expressed as µmol H2O2 equivalents/L and mmol Trolox equiv./L respectively. The overall oxidative stress index (OSI) was subsequently calculated as the ratio of TOS to TAR. To evaluate systemic lipid peroxidation, malondialdehyde (MDA) concentrations (nmol/mL) were measured using the thiobarbituric acid assay. Concurrently, total serum thiols (SH) were measured as an index of systemic antioxidant reserve, expressed in µmol/L. Lastly, systemic nitric oxide (NO) production was indirectly determined by quantifying its stable end-products (nitrates and nitrites, NOx) via the Griess reaction, with final results reported in µmol/L. All spectrophotometric analyses were executed in triplicate to ensure reliability.

Statistical analysis

All statistical analyses were performed using IBM SPSS Statistics software, version 20.0 (IBM, Armonk, NY, USA). Because macroscopic cartilage scores are ordinal and histological extracellular matrix quantifications (Collagen I and III percentages) demonstrated non-normal distributions, descriptive statistics for these variables are presented as the median and interquartile range [Q1, Q3]. Oxidative stress parameters are reported as mean (± standard deviation). Normality was assessed for each continuous variable using the Shapiro–Wilk test, and

homogeneity of variance was assessed using Levene's test where relevant. For normally distributed data with homogeneous variance, inter-group comparisons were performed using one-way analysis of variance (ANOVA), followed by Dunnett's test for comparisons against the control cohort and Tukey's HSD test for all pairwise group comparisons. For normally distributed data with unequal variance across groups, Welch's ANOVA was used, followed by the Games-Howell post-hoc test. Non-normally distributed continuous data and ordinal scoring systems were analyzed using non-parametric methods: the Wilcoxon matched-pairs signed-rank test was applied for intra-animal paired-knee comparisons, and for inter-group analyses the Kruskal-Wallis test, followed by pairwise Mann-Whitney U tests for multiple comparisons, with Holm-Bonferroni correction. A p-value of $p < 0.05$ was considered statistically significant. The matched-pairs rank-biserial correlation (RBC) was calculated as an effect size estimate for the Wilcoxon signed-rank tests, based on the proportion of favorable to unfavorable rank sums.

The pilot control cohort (3 animals, both knees scored) was represented by a single value per animal — the higher (worse) of the two knee macroscopic scores respectively the mean of the histological extracellular matrix quantifications — yielding three independent observations for between-group comparisons, avoiding pseudoreplication.

Post-hoc statistical power was estimated via bootstrap resampling: 10,000 samples were drawn with replacement from the observed data and tested using the corresponding non-parametric test, with power calculated as the proportion of resamples yielding $p < 0.05$ in Python (v3.12.3) using SciPy (v1.17.1) and NumPy (v2.4.4). A p-value < 0.05 was considered statistically significant.

Results

Macroscopic evaluation of articular cartilage

Macroscopic evaluation demonstrated an overall trend toward reduced cartilage degeneration in treated knees relative to their paired untreated controls. Representative macroscopic findings are shown in figure 1. This paired reduction reached statistical significance, following correction for multiple comparisons, in the MFAT+HA and MFAT+COL groups (Wilcoxon signed-rank, adjusted $p = 0.047$ for both); the MFAT group showed an identical direction of effect but did not reach significance after correction ($p = 0.063$). RBC was 1.0 in all three groups, indicating uniform direction of effect among informative pairs; this describes effect consistency, not statistical significance, and does not establish a confirmed treatment effect in the MFAT group given $p = 0.063$.

When treated knees were compared against the pilot control cohort all three treatment groups showed lower macroscopic scores using the Mann-Whitney U test (MFAT, $p = 0.048$; MFAT+HA, $p = 0.017$; MFAT+COL, $p = 0.017$), and this held after Holm-Bonferroni correction, though at the threshold for significance (adjusted $p = 0.050$ for all three) (Figure 2).

Post-hoc power for the MFAT comparison was 34% at the observed sample size ($n = 6$), compared to >99% for MFAT+HA and MFAT+COL ($n = 7$ each).

No significant differences were observed among the three treatment groups ($p = 0.57$). As this omnibus test did not reach significance, pairwise inferential comparisons were not performed, and RBC are reported descriptively only, to characterize the magnitude of separation between arms (MFAT vs. MFAT+HA, RBC=0.19; MFAT vs. MFAT+COL, RBC=−0.05; MFAT+HA vs. MFAT+COL, RBC=0.29). Untreated knees did not differ significantly across groups ($p = 0.51$), supporting comparable baseline severity of osteoarthritic change at the time of evaluation.

A more prominent synovial reaction was qualitatively observed in the MFAT+HA group during gross examination. Tibial osteophytosis was a prevalent macroscopic finding in the untreated joints; in contrast, the treated knees exhibited an attenuated osteogenic response, characterized by a visible reduction in both osteophyte volume and morphological prominence.

Collagen birefringence analysis

Semi-quantitative analysis of representative PSR–stained sections under polarized light showed no significant differences in %Collagen I between treated and untreated knees in any group, nor between treated knees and the control cohort. No significant differences in collagen III were observed in the MFAT or MFAT+HA groups.

Only the MFAT+COL group demonstrated a significant increase in collagen III-positive birefringence compared with paired untreated knees (adjusted $p = 0.047$). This increase did not survive correction for multiple comparisons when MFAT+COL was instead compared against the control cohort (adjusted $p = 0.050$), and the preceding omnibus test for this comparison did not reach significance ($p = 0.052$) (Figure 3). The omnibus test found no significant difference among treatment groups for either marker. Representative images of the corresponding PSR-stained sections under polarized light are shown in figure 4. Post-hoc power was low for %Collagen I across all comparisons (3–35%), and for %Collagen III vs. control in the MFAT and MFAT+HA groups (9–10%), indicating this study was likely underpowered to detect effects of this outcome measure at conventional sample sizes, independent of whether a true effect exists. For %Collagen III, paired-comparison power was 9% for MFAT, 35% for MFAT+HA. Power exceeded 95% only for %Collagen III in the MFAT+COL group, reflecting the substantially larger effect size observed specifically in that comparison.

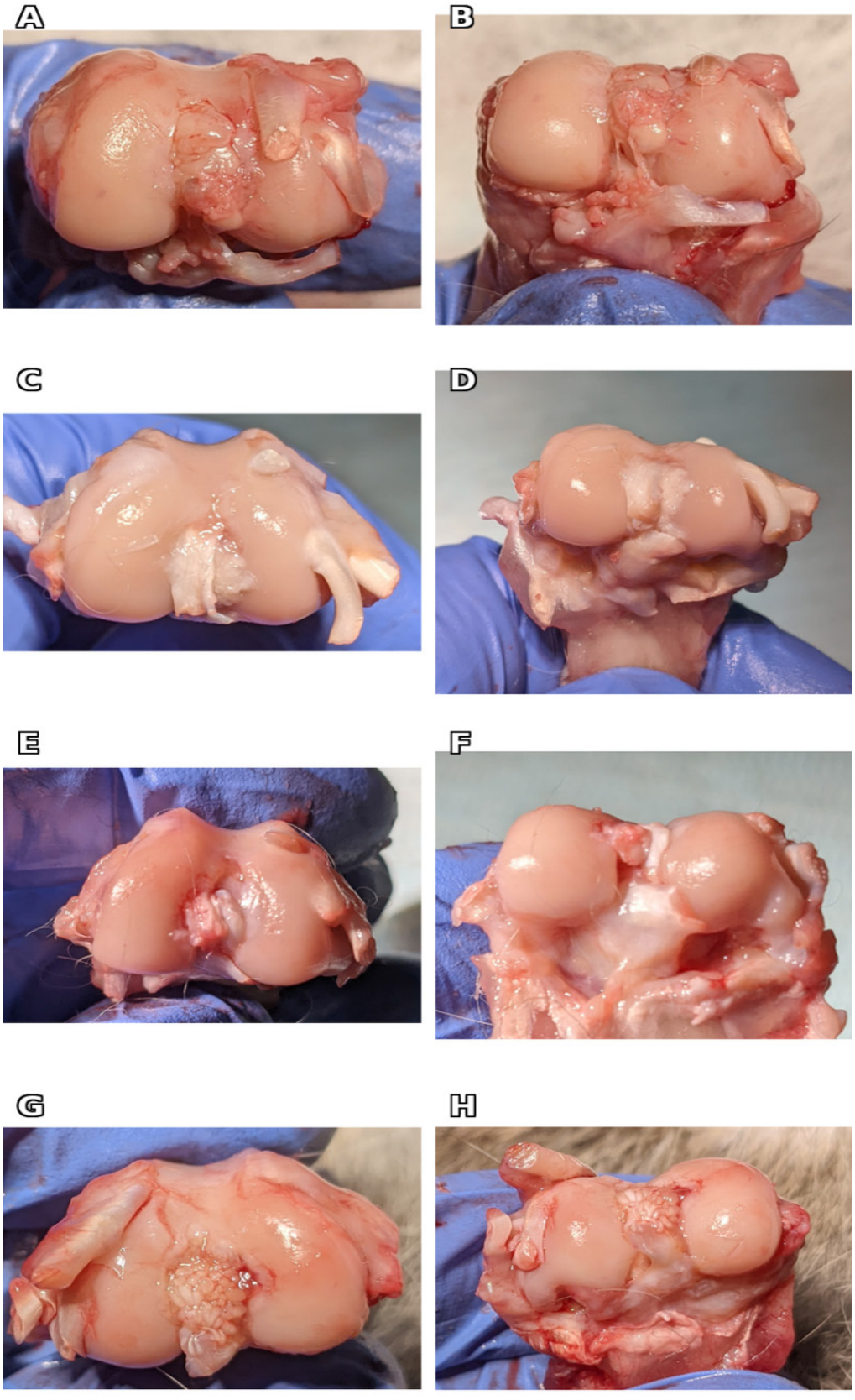

Figure 1. Representative macroscopic images of femoral condyles within each group: MFAT (A,B), MFAT+HA (C,D), MFAT+COL (E,F), control (G,H). MFAT=microfragmented adipose tissue; HA=hyaluronic acid; COL=collagen.

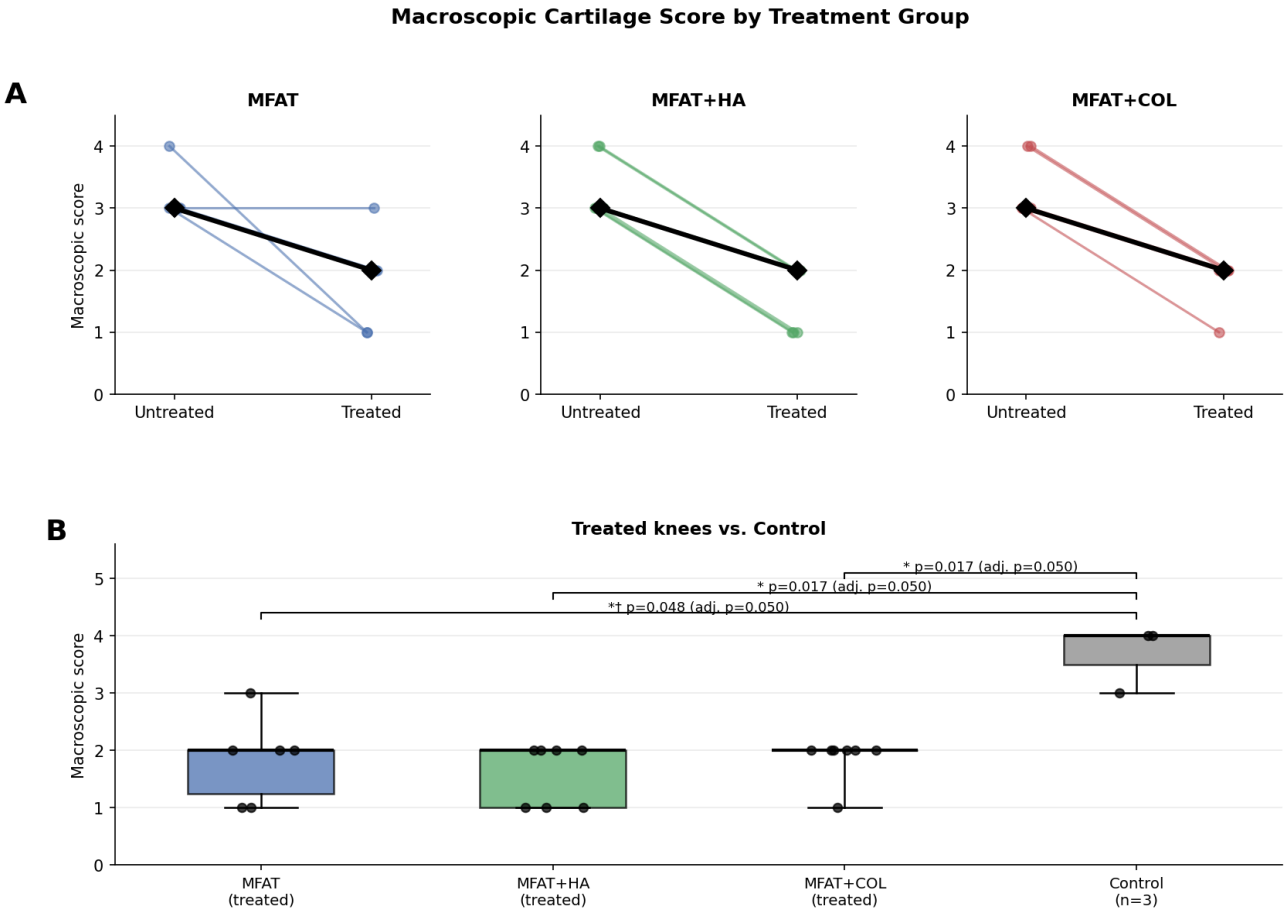

Figure 2. Macroscopic evaluation of cartilage degeneration following intra-articular MFAT-based treatment. (A) Paired macroscopic scores of untreated versus treated knees within each treatment group (MFAT(n=6), MFAT+HA(n=7), MFAT+COL(n=7)), the black line with diamond markers indicates the group median. (B) Macroscopic scores of treated knees from each group compared with the untreated pilot control cohort. Box-plots show median and interquartile range [Q1, Q3]; *p < 0.05. MFAT=microfragmented adipose tissue; HA=hyaluronic acid; COL=collagen.

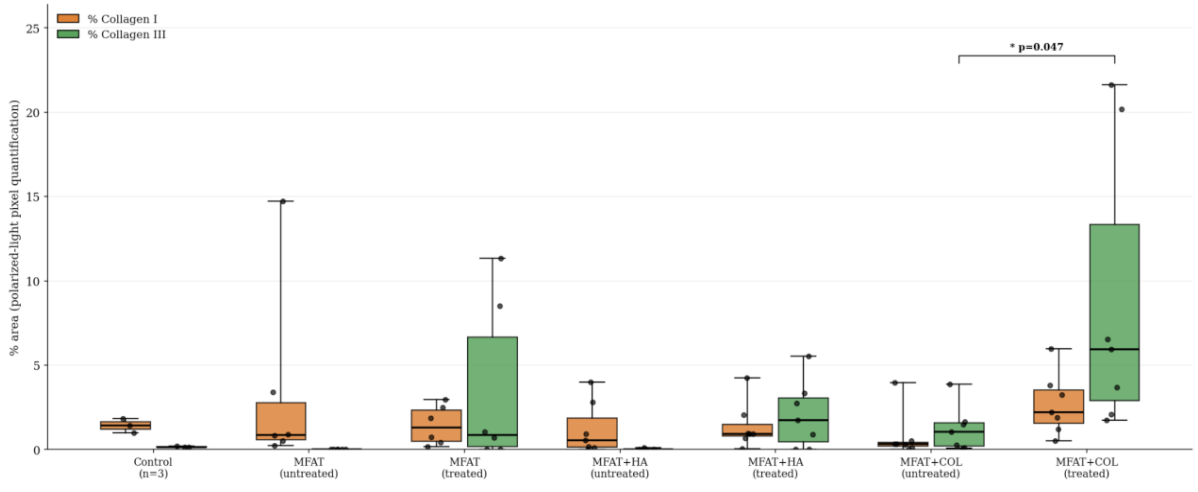

Figure 3. Percentage area of type I (orange) and type III (green) collagen, quantified by polarized-light pixel analysis of Picrosirius Red–stained sections, in untreated and MFAT-treated knees for each group and in the pilot control cohort. Box-plots show median [Q1, Q3]; *p < 0.05 vs. paired control. MFAT=microfragmented adipose tissue; HA=hyaluronic acid; COL=collagen.

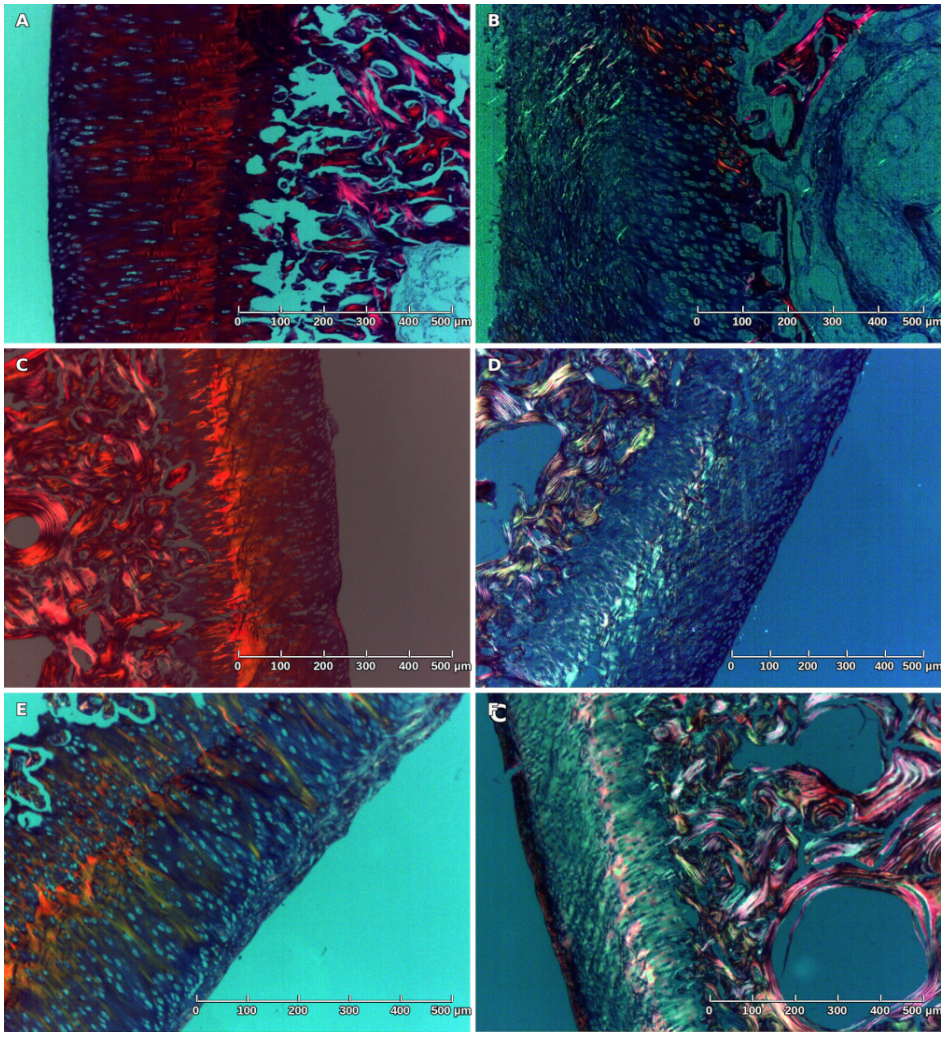

Figure 4. Representative polarized light microscopy images. Untreated versus treated knee cartilage collagen birefringence across MFAT-based treatment groups. Representative Picrosirius Red–stained sections under polarized light microscopy, paired by group: untreated (A, C, E) and treated (B, D, F) knees for MFAT (A, B), MFAT+HA (C, D), and MFAT+COL (E, F). Orange-red birefringence associated with thick, densely packed fibers; green birefringence associated with thin, loosely packed fibers. MFAT=microfragmented adipose tissue; HA=hyaluronic acid; COL=collagen.

Serum oxidative stress analysis

For each experimental group, the mean (± standard deviation) of oxidative stress parameters is reported in figure 5. TOS and OSI were each significantly elevated in the MFAT (p=0.024, p=0.023) and MFAT+HA (p=0.013, p=0.013) groups relative to control; neither differed significantly in MFAT+COL. Total thiols did not differ significantly between any treated group and control, but were significantly lower in MFAT+HA relative to MFAT alone (adjusted p=0.031). MDA was nominally higher in the MFAT (p = 0.0085) and MFAT+HA (p = 0.0046) groups relative to control by Games-Howell post-hoc following Welch's ANOVA. This did not replicate under the non-parametric Kruskal-Wallis/Mann-Whitney approach used for the other markers, and given the three-animal control group, we regard it as a statistically fragile signal rather than a confirmed group difference.

TAR was comparable across groups. Nitric oxide was significantly lower in all three treated groups relative to control (p<0.0001) — the only marker to reach significance across every treatment arm and to remain significant after correction across all six markers. No significant differences were observed between treatment groups for any other marker, with the exception of total thiols. Given the small group sizes, particularly the three-animal control cohort, these findings should be interpreted as directionally consistent signals rather than fully confirmed effects.

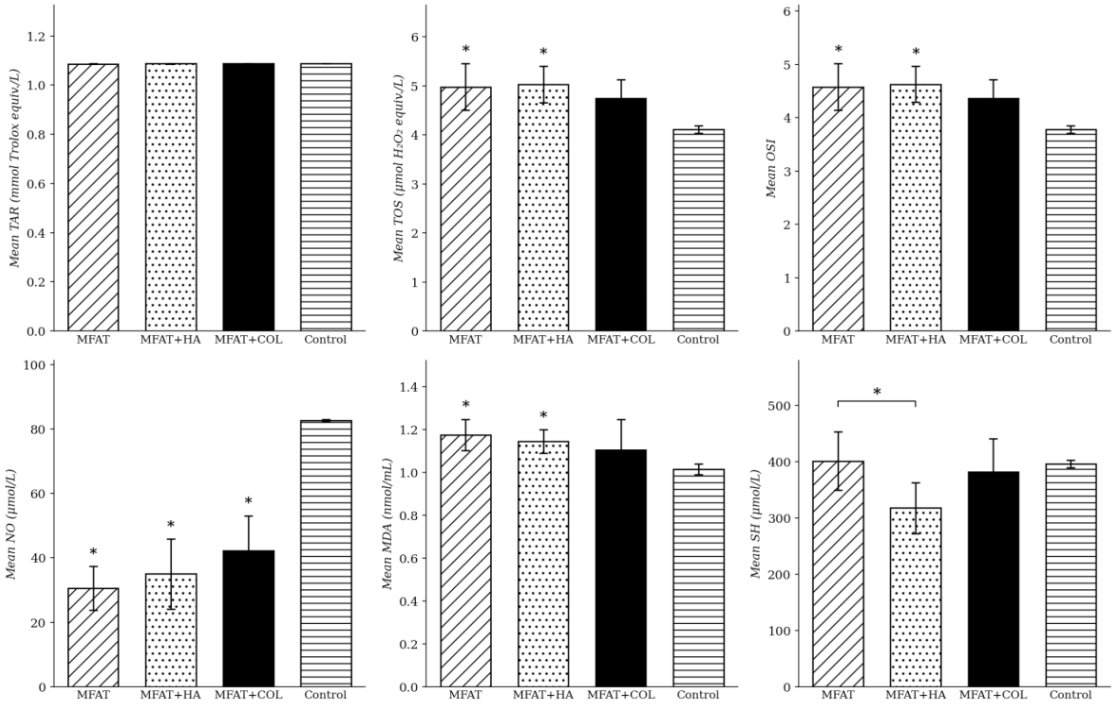

Figure 5. Mean levels (± standard deviation) of oxidative stress parameters in serum in MFAT(n=6), MFAT+HA(n=7), and MFAT+COL(n=7) groups compared with the pilot control cohort(n=3). *p < 0.05 vs. Control. TOS = total oxidative status; TAR = total antioxidant response; OSI = oxidative stress index; MDA = malondialdehyde; SH = total serum thiols; NO = nitric oxide, MFAT=microfragmented adipose tissue; HA=hyaluronic acid; COL=collagen.

Discussion

Macroscopic evaluation demonstrated an overall structural benefit of the interventions, with treated knees exhibiting reduced cartilage degeneration relative to their paired internal controls. While this paired improvement reached statistical significance only in the MFAT+HA and MFAT+COL groups, the MFAT-only group followed an identical trend. Furthermore, all three treatments produced macroscopic cartilage scores that were significantly lower than those of the pilot control cohort, though this difference remained at the strict threshold of significance following correction for multiple comparisons. This result must be interpreted with appropriate caution: the control cohort comprised only three independent animals, which limited the precision of the baseline characterization and inherently constrained the achievable statistical power. Nevertheless, the directional concordance observed in the intra-animal paired analyses—where informative observations uniformly moved toward structural improvement — describes the consistency of effect direction, not statistical significance, and does not by itself establish a confirmed treatment effect in the MFAT group, where the paired comparison did not reach significance. Ultimately, a larger, contemporaneously recruited control cohort is needed to confirm these findings with greater statistical confidence. The magnitude of the pairwise rank-biserial correlations between treatment arms (RBC ≤ 0.29) suggests that any true difference among the three treatment strategies is, at most, modest, and that its reliable detection would require substantially larger group sizes. Accordingly, the non-significant omnibus result should be interpreted as inconclusive with respect to relative treatment efficacy, rather than as evidence of true equivalence among the MFAT, MFAT+HA, and MFAT+COL groups. At the histological level, MFAT combined with injectable collagen was distinctly associated with increased thin, loosely packed–predominant birefringence relative to its paired untreated knee, a pattern not observed with MFAT alone or MFAT+HA. NO was significantly lower in all three treated groups relative to control, the only oxidative stress marker to reach significance across every treatment arm, while TOS and OSI were each significantly elevated in the MFAT and MFAT+HA groups relative to control.

Minimally manipulated adipose-derived therapies, particularly SVF and MFAT, have emerged as prominent regenerative interventions [6]. Traditional SVF isolation relies on enzymatic digestion via collagenase to separate mature adipocytes from stromal cellular components [7]. While effective for cell expansion, the potential for residual enzyme contamination in injectable clinical products

poses significant safety risks and can trigger adverse patient reactions [8]. To circumvent these safety concerns, MFAT is generated utilizing mechanical disruption and micro-filtration [8]. Although mechanical extraction was historically associated with lower cellular yields due to the resilient bonds between adipocytes and collagen, contemporary filtration and emulsification protocols effectively overcome this limitation, allowing for a high cell yield without the risks associated with enzymatic digestion [7]. A critical distinction between MFAT and enzymatically derived SVF is MFAT's preservation of the native extracellular matrix and intact microvascular architecture [16]. Retaining this perivascular niche provides a natural structural scaffold that enhances cellular survival, migration, and complex intercellular signaling [16]. The therapeutic efficacy of these tissues is primarily driven by the paracrine and immunomodulatory functions of their cellular constituents [17]. Adipose-derived stem cells (ADSCs) and endothelial progenitors within the adipose tissue secrete a robust profile of bioactive molecules, cytokines, and growth factors. These secretions modulate the local articular microenvironment and regulate immune responses, thereby shifting the joint ecosystem toward a pro-regenerative, anti-inflammatory state [18].

Extensive preclinical in vivo studies consistently corroborate the chondroprotective and anti-inflammatory capacity of minimally manipulated adipose therapies. In rodent models of induced OA, both SVF and MFAT have demonstrated the ability to maintain histological cartilage integrity by downregulating matrix-degrading enzymes (MMPs) and reducing systemic inflammatory cytokines, such as IL-1β and IL-6 [19,20]. In rabbit OA models, SVF mitigates cartilage degeneration by balancing anabolic and catabolic factors, while MFAT specifically promotes a robust anti-inflammatory environment characterized, prolonged synovial biodistribution and enhanced long-term cellular survival [21,22]. Furthermore, investigations utilizing sheep OA models indicate that while isolated ADSCs may offer superior direct cartilage matrix production [23], intact adipose fractions (SVF/MFAT) demonstrate superior efficacy in actively counteracting the inflammatory microenvironment [24].

In healthy joints, endogenous HA exists at a high molecular weight, providing essential viscoelasticity and mechanical support. However, as osteoarthritis progresses, HA undergoes progressive depolymerization, significantly compromising the lubrication and shock-absorbing properties of the synovial fluid [9]. The intra-articular administration of exogenous HA aims to counteract this decline. Mechanically, HA restores the rheological environment; biologically, it modulates inflammatory pathways, stimulates proteoglycan synthesis, and regulates chondrocyte metabolism [9]. The clinical efficacy of exogenous HA is highly dependent on its molecular weight. High molecular weight (HMW) and cross-linked formulations are associated with superior viscoelastic properties, prolonged intra-articular residence time, and enhanced interactions with CD44 receptors on chondrocytes and synoviocytes [25]. These properties allow HMW HA to more effectively downregulate catabolic enzymes (such as MMP-13) and inflammatory markers, ultimately translating to sustained structural protection and durable symptom relief without the need for frequent re-administration [10].

Furthermore, emerging evidence highlights the synergistic potential of combining HA with other biological and regenerative agents. While HA effectively stabilizes the viscoelastic environment and offers baseline anti-inflammatory benefits, pairing it with advanced orthobiologics—such as cellular therapies, platelet-rich plasma, or targeted peptides—amplifies therapeutic efficacy through complementary mechanisms. In these combinatorial approaches, HA acts as a protective, lubricating scaffold that modulates the joint microenvironment and reduces oxidative stress, thereby facilitating the active tissue regeneration and chondrogenesis driven by the primary biologic agent [25].

While HA predominantly functions by restoring the viscoelasticity of the synovial fluid to provide mechanical lubrication and anti-inflammatory effects [26], intra-articular collagen injections offer a distinct, dual-mechanism approach by delivering both symptomatic relief and delay in cartilage degeneration [27,28]. As the primary structural protein comprising up to 75% of the cartilage extracellular matrix (ECM) dry weight, collagen formulations possess regenerative properties [10]. In vitro and preclinical animal studies demonstrate that exposure to various collagen preparations directly stimulates chondrocyte proliferation, upregulates endogenous HA and ECM protein synthesis, and significantly suppresses the release of pro-inflammatory mediators [10]. In surgically induced rabbit models of osteoarthritis, the intra-articular administration of these collagen scaffolds has been shown to successfully delay cartilage degeneration and promote the histological restoration of the articular surface [28]. These biological and structural benefits are increasingly corroborated by emerging clinical evidence. Randomized controlled trials indicate that collagen therapies deliver functional symptom relief comparable to standard HA at early intervals, while sustaining significant clinical improvements up to 24 weeks post-treatment, positioning collagen as a highly viable biological adjuvant for actively mitigating cartilage degradation [27].

The strategy of combining minimally manipulated adipose tissue with structural adjuvants, such as HA, is rooted in the synergistic interplay between biological immunomodulation and biomechanical scaffolding. As demonstrated by Svolacchia et al. [29] in soft tissue regeneration for the correction of deep wrinkles, HA

serves as a durable, highly viscous matrix that anchors adipose-derived progenitors at the target site, enhancing the overall regenerative process. Furthermore, their work highlighted the critical importance of tissue microfiltration; by actively eliminating fibrous shoots and cellular debris from the lipoaspirate, the therapeutic quality of the cellular graft is optimized, specifically by preventing the activation of inflammatory cascades via the Toll-like receptor system. In the context of joint pathology, Lv et al. [23] corroborated the clinical utility of this dual approach, noting that administration of the heterogeneous cell populations of the SVF alongside HA yields significant functional improvements, alleviates pain, and promotes MRI-confirmed cartilage regeneration in OA patients. Their preclinical large-animal model further indicates that the addition of an HA scaffold to adipose-derived cellular therapies provides a vital supportive niche that effectively blocks osteoarthritis progression. Consequently, coupling a cell-rich adipose fraction with a robust structural biomaterial aims to simultaneously neutralize local tissue inflammation while providing the necessary mechanical support for sustained structural repair.

Evaluation of the extracellular matrix utilizing PSR microscopy revealed a preponderance of thick, highly aligned collagen bundles within the untreated osteoarthritic lesions in the control, MFAT and MFAT+HA groups. This structural profile suggests the formation of fibrocartilaginous repair tissue rather than the typical architecture of native hyaline cartilage [13]. Conversely, the treated joints demonstrated a shift toward birefringence patterns typically associated with thinner, loosely packed fibers — showing a nominally significant paired difference in the MFAT+COL cohort that did not survive correction for multiple comparisons against the control cohort, with a similar, non-significant trend evident in the MFAT and MFAT+HA groups. This structural shift might suggest an active, ongoing phase of extracellular matrix remodeling, a regenerative process potentially amplified by the injectable collagen adjuvant. Importantly, the interpretation of these histological findings warrants methodological caution. The color spectrum produced during PSR birefringence is highly sensitive to physical variables, including intrinsic fiber thickness, spatial orientation, and optical alignment under polarized light [14]. Therefore, this semi-quantitative analysis should be regarded as a broad indicator of overall matrix architecture and dynamic tissue turnover, rather than a definitive molecular quantification of specific collagen subtypes.

The modulation of systemic and local oxidative stress following joint-specific interventions has been previously documented across various preclinical models. For instance, in a rabbit model of early temporomandibular joint osteoarthritis, Erdayandi et al. [30] demonstrated that the intra-articular administration of daidzein (a polyphenolic isoflavone structurally similar to mammalian estrogen 17-β-estradiol) significantly reduced systemic TOS and OSI, while the TAR remained unaltered between the experimental and control groups. Similarly, Mehak et al. [31] observed a dose-dependent improvement in TOS following the administration of a chondroprotective agent (pomegranate seed oil) in a papain-induced rat model of knee osteoarthritis.

Furthermore, MDA serves as a primary terminal byproduct of lipid peroxidation and a widely validated biomarker for oxidative stress in joint pathology [32]. Elevated MDA concentrations are consistently associated with the structural progression of osteoarthritis across species, having been observed in canine models by Goranov et al [33] as well as in the synoviocytes of human osteoarthritic patients compared to healthy controls [34]. Targeted therapeutic interventions have been shown to successfully inhibit this process; for example, Bai et al. [32] reported that a 6-week treatment protocol (Danshen, Salvia miltiorrhiza, a traditional Chinese medicine) in an osteoarthritic rabbit model markedly depleted the abnormally elevated MDA levels within both the synovium and articular cartilage, effectively suppressing local lipid peroxidation.

Systemic oxidative stress profiling demonstrated elevated TOS and OSI in the MFAT and MFAT+HA cohorts relative to the untreated baseline control, both reaching statistical significance. MDA followed the same direction but on weaker footing: the Games-Howell result was nominally significant, but as noted above this did not replicate under non-parametric testing and likely reflects the instability of variance estimates in the three-animal control group rather than a robust group difference. We therefore treat the MDA signal as suggestive, unlike the TOS and OSI findings. This systemic oxidative shift may be attributable to the biological integration and paracrine activity of the administered human-derived xenograft within the joint space. It is hypothesized that the introduction of a cross-species tissue matrix could initiate a localized immune recognition response, but this transient elevation may also be reflective of the active cellular remodeling phase initiated by the orthobiologic therapies. It is possible that MFAT administration promotes local macrophage recruitment for debris clearance and matrix synthesis, and that the associated ROS generation contributes to the elevated systemic TOS observed in treated groups; however, this mechanism was not directly assessed, and the present data cannot distinguish a functional repair-associated oxidative burst from a pathological stress response.

This mechanism remains hypothetical and was not directly tested in the present study. The concomitant reduction in total serum thiols observed in the MFAT+HA group relative to MFAT alone — though not relative to control — may be compatible with such a process,

but could equally reflect other, unmeasured sources of systemic redox perturbation. In the absence of immunological or metabolic data specifically designed to test this mechanism, it should be regarded as a plausible explanation warranting dedicated investigation rather than an established finding. Serum thiols function as a primary systemic antioxidant reserve, scavenging free radicals to maintain redox homeostasis [35]. As noted during macroscopic evaluation, the addition of high-molecular-weight hyaluronic acid provoked a more pronounced local synovial reaction. It is hypothesized that the enhanced viscoelastic properties and extended intra-articular retention of the HA matrix prolonged the localized immunomodulatory response. This sustained cellular activity may have subsequently increased the consumption of the systemic thiol pool required to buffer the associated oxidative output.

Despite the observed elevations in TOS, OSI, and MDA, the systemic concentration of NO — a potent nitrosative and pro-inflammatory mediator implicated in osteoarthritis pathogenesis [36] — was significantly reduced across all three treatment arms compared to the control group. This finding could suggest that localized therapeutic intervention may attenuate the primary source of joint-derived NO production. Taken together, the oxidative stress profile in this study was mixed rather than uniformly favorable: NO was the only marker reduced in every treated group, while TOS, OSI, and MDA moved in the opposite direction in MFAT and MFAT+HA. These findings should not be read as evidence of a net beneficial systemic oxidative stress effect of MFAT-based treatment. Consequently, by reducing the structural disease burden at the articular level MFAT-based therapy may exert systemic biological effects beyond local cartilage preservation. Notably, MFAT+COL did not differ significantly from control on any general oxidative markers (TOS, OSI, MDA, TAR, or thiols), distinguishing it from MFAT and MFAT+HA. This may reflect a distinct biological effect localized to collagen-driven matrix remodeling rather than a systemic oxidative response, but could also reflect its different administration schedule; the present design cannot distinguish between these possibilities.

The utilization of human-derived MFAT in a lapine osteoarthritis model was selected due to both structural and translational considerations. Rabbit adipose tissue is characterized by a denser, highly fibrotic stromal architecture compared to human fat, which impedes standardized mechanical micro-fragmentation and yields a product that does not accurately reflect the clinical reality of the adipose tissue micro-fragmentation system. Furthermore, employing human lipoaspirate enabled the targeted evaluation of site-specific tissue depots—specifically, the knee fat pad and the peritrochanteric region—which are known to harbor distinct regenerative and cellular profiles. Finally, the intra-articular administration of human adipose-derived xenografts is a validated approach previously established in preclinical literature [37–39].

This study possesses several methodological strengths. The implementation of a paired design, utilizing the contralateral untreated joint as an internal control, significantly minimized inter-subject biological variance and strengthened the reliability of the local therapeutic outcomes. Additionally, the use of arthroscopic ACLT allowed for a standardized, minimally invasive induction of the osteoarthritis model, reducing confounding periarticular surgical trauma. The research also benefited from a multifaceted assessment strategy that integrated macroscopic evaluation, histological matrix analysis, and systemic biochemical profiling. Furthermore, the therapeutic interventions utilized a clinically relevant, purely mechanical MFAT preparation protocol derived from human lipoaspirate, accurately reflecting real-world clinical processing and tissue heterogeneity.

However, several limitations must be acknowledged. The primary constraint is the small sample size, which limited the statistical power to detect subtle inter-group differences, particularly concerning the secondary structural adjuvants and the systemic oxidative stress correction thresholds. The 12-week follow-up duration is relatively short, precluding the assessment of long-term graft viability, sustained extracellular matrix integration, or late-stage joint degeneration. Furthermore, the administration of human-derived MFAT into a rabbit model constitutes a xenograft approach. We did not perform in this study any direct immunological assessment — including immune-cell infiltration, anti-human immune responses— and cannot therefore determine whether the observed systemic oxidative stress changes reflect a xenogeneic immune response, the biological activity of the graft itself, or another mechanism. In addition, HA and collagen were administered according to each product's manufacturer-recommended clinical schedule, resulting in a single administration for HA (week 8) versus two administrations for collagen (weeks 8 and 10]. This asymmetry can influence direct comparison between the MFAT+HA and MFAT+COL groups.

Direct immunological characterization of the local and systemic response to xenogeneic MFAT is a priority for future studies. Finally, the evaluation of the extracellular matrix was restricted to semi-quantitative PSR birefringence to assess collagen architecture. The absence of histopathological scoring, targeted immunohistochemistry and molecular gene expression profiling restricts a definitive molecular characterization and functional assessment of the load-bearing capacity of the repaired articular surfaces. Because osteoarthritis is clinically relevant primarily through functional impairment, the absence of gait analysis and weight-bearing distribution limits the translational significance

of the structural findings and represents an important direction for future studies.

Conclusions

In this experimental rabbit OA model, intra-articular MFAT attenuated structural cartilage degeneration in the presence of uncorrected mechanical joint instability. The systemic oxidative stress profile was mixed rather than uniformly favorable: nitric oxide was reduced across all treated groups, whereas TOS, OSI, and MDA were elevated in the MFAT and MFAT+HA groups relative to control. These findings do not support a net beneficial systemic oxidative stress effect of MFAT-based treatment and warrant further mechanistic investigation. The addition of injectable collagen was associated with a shift in PSR birefringence patterns that may reflect extracellular matrix remodeling, though this did not survive correction for multiple comparisons and should be interpreted as hypothesis-generating rather than confirmatory, whereas hyaluronic acid did not provide additional structural benefit under the present experimental conditions. These findings support further investigation of MFAT-based therapies in larger preclinical studies and carefully designed clinical trials.

AI assistance disclosure

During the preparation and revision of this manuscript, AI-assisted tools were used to graphically exemplify the statistical data. Specifically, Claude (Anthropic, Claude Sonnet 5, 2026) was utilized to generate visual representations and format the graphs based on the provided datasets. All raw data, scientific content, statistical methodology, and conclusions were generated solely by the authors. All AI-assisted graphical outputs were reviewed, verified, and approved by the authors, who accept full responsibility for the accuracy, integrity, and originality of the manuscript's figures and overall content.

Aknowledgements

The authors would like to thank Teodora-Irina Adam-Bonci and Ana Uifălean from the Pathophysiology Department of Iuliu Hatieganu University of Medicine and Pharmacy Cluj-Napoca, Romania, Anca Jurj from Genomics Department of MEDFUTURE — Institute for Biomedical Research, Iuliu Hatieganu University of Medicine and Pharmacy and Sebastian Lupu for technical support during manuscript writing.

Authors' contributions

Conceptualization, A.O.A., H.R.C.B., L.-M.G., D.O.-D. and M.C.; methodology, A.O.A, H.R.C.B., D.A. and L.-M.G.; data curation, A.O.A., D.G..; formal analysis, A.O.A. and D.G.; writing – original draft, A.O.A. and M.C.; writing—review & editing, A.O.A. and H.R.C.B.; supervision, D.A., D.O.-D. and M.C. All authors have read and agreed to the published version of the manuscript.

References

1. Campos WNS, Souza MA, Ruiz T, Peres TP, Néspoli PB, Marques ATC, et al. Experimental osteoarthritis in rabbits: lesion progression. Pesqui Veterinária Bras. 2013;33:279–285.
2. Wang Y, Tang X, Peng JR, Deng Y, Lan S, Yen Y, et al. Global, regional, and national burden of osteoarthritis among middle-aged and older adults: estimates from the global burden of disease study 2021 and projections to 2050. Front Med (Lausanne). 2025;12:1696929. doi: 10.3389/fmed.2025.1696929.
3. Zaripova L, Tazhibayeva D, Kabdualieva N, Aitbayeva Z, Beglarova G, Yermentayeva L, et al. Osteoarthritis: A contemporary view of the problem, the possibilities of therapy and prospects for further research. J Clin Med Kazakhstan. 2022;19:6–12.
4. Zhu C, Wu W, Qu X. Mesenchymal stem cells in osteoarthritis therapy: a review. Am J Transl Res. 2021;13:448-461.
5. Lindroos B, Suuronen R, Miettinen S. The potential of adipose stem cells in regenerative medicine. Stem Cell Rev Rep. 2011;7:269-291. doi: 10.1007/s12015-010-9193-7.
6. Adam AO, Benea HRC, Fotescu HM, Alcalá Ruiz M, Cimpean GC, Ciornei V, et el. Recent Trends in Adipose Tissue-Derived Injectable Therapies for Osteoarthritis: A Scoping Review of Animal Models. Medicina (Kaunas). 2024;60:707. doi: 10.3390/medicina60050707.
7. Lana JFSD, Lana AVSD, da Fonseca LF, Coelho MA, Marques GG, Mosaner T, et al. Stromal Vascular Fraction for Knee Osteoarthritis - An Update. J Stem Cells Regen Med. 2022;18:11-20. doi: 10.46582/jsrm.1801003.
8. Schipper JAM, van Laarhoven CJHCM, Schepers RH, Tuin AJ, Harmsen MC, Spijkervet FKL, et al. Mechanical Fractionation of Adipose Tissue-A Scoping Review of Procedures to Obtain Stromal Vascular Fraction. Bioengineering (Basel). 2023;10:1175. doi: 10.3390/bioengineering10101175.
9. Chavda S, Rabbani SA, Wadhwa T. Role and Effectiveness of Intra-articular Injection of Hyaluronic Acid in the Treatment of Knee Osteoarthritis: A Systematic Review. Cureus. 2022;14:e24503. doi: 10.7759/cureus.24503.
10. Tarantino D, Mottola R, Palermi S, Sirico F, Corrado B, Gnasso R. Intra-Articular Collagen Injections for Osteoarthritis: A Narrative Review. Int J Environ Res Public Health. 2023;20:4390. doi: 10.3390/ijerph20054390.
11. He Y, Li Z, Alexander PG, Ocasio-Nieves BD, Yocum L, Lin H, Tuan RS. Pathogenesis of Osteoarthritis: Risk Factors, Regulatory Pathways in Chondrocytes, and Experimental Models. Biology (Basel). 2020;9:194. doi:

10.3390/biology9080194.

12. Laverty S, Girard CA, Williams JM, Hunziker EB, Pritzker KP. The OARSI histopathology initiative - recommendations for histological assessments of osteoarthritis in the rabbit. Osteoarthritis Cartilage. 2010;18 Suppl 3:S53-65. doi: 10.1016/j.joca.2010.05.029.
13. Yoshioka NK, Young GM, Khajuria DK, Karuppagounder V, Pinamont WJ, Fanburg-Smith JC et al. Structural changes in the collagen network of joint tissues in late stages of murine OA. Sci Rep. 2022;12:9159. doi: 10.1038/s41598-022-13062-y.
14. López De Padilla CM, Coenen MJ, Tovar A, De la Vega RE, Evans CH, Müller SA. Picrosirius Red Staining: Revisiting Its Application to the Qualitative and Quantitative Assessment of Collagen Type I and Type III in Tendon. J Histochem Cytochem. 2021;69:633-643. doi: 10.1369/00221554211046777.
15. Adam-Bonci TI, Bonci EA, Pârvu AE, Herdean AI, Moț A, Taulescu M, et al. Vitamin D Supplementation: Oxidative Stress Modulation in a Mouse Model of Ovalbumin-Induced Acute Asthmatic Airway Inflammation. Int J Mol Sci. 2021;22:7089. doi: 10.3390/ijms22137089.
16. Ude CC, Shah S, Ogueri KS, Nair LS, Laurencin CT. Stromal Vascular Fraction for Osteoarthritis of the Knee Regenerative Engineering. Regen Eng Transl Med. 2022;8:210-224. doi: 10.1007/s40883-021-00226-x.
17. Xu T, Yu X, Yang Q, Liu X, Fang J, Dai X. Autologous Micro-Fragmented Adipose Tissue as Stem Cell-Based Natural Scaffold for Cartilage Defect Repair. Cell Transplant. 2019;28:1709-1720. doi: 10.1177/0963689719880527.
18. Molnar V, Pavelić E, Vrdoljak K, Čemerin M, Klarić E, Matišić V, et al. Mesenchymal Stem Cell Mechanisms of Action and Clinical Effects in Osteoarthritis: A Narrative Review. Genes (Basel). 2022;13:949. doi: 10.3390/genes13060949.
19. Muñoz-Criado I, Meseguer-Ripolles J, Mellado-López M, Alastrue-Agudo A, Griffeth RJ, Forteza-Vila J, Cugat R, et al. Human Suprapatellar Fat Pad-Derived Mesenchymal Stem Cells Induce Chondrogenesis and Cartilage Repair in a Model of Severe Osteoarthritis. Stem Cells Int. 2017;2017:4758930. doi: 10.1155/2017/4758930.
20. Ohashi H, Nishida K, Yoshida A, Nasu Y, Nakahara R, Matsumoto Y, et al. Adipose-Derived Extract Suppresses IL-1β-Induced Inflammatory Signaling Pathways in Human Chondrocytes and Ameliorates the Cartilage Destruction of Experimental Osteoarthritis in Rats. Int J Mol Sci. 2021;22:9781. doi: 10.3390/ijms22189781.
21. Filardo G, Tschon M, Perdisa F, Brogini S, Cavallo C, Desando G, et al. Micro-fragmentation is a valid alternative to cell expansion and enzymatic digestion of adipose tissue for the treatment of knee osteoarthritis: a comparative preclinical study. Knee Surg Sports Traumatol Arthrosc. 2022;30:773-781. doi: 10.1007/s00167-020-06373-y.
22. Desando G, Bartolotti I, Martini L, Giavaresi G, Nicoli Aldini N, Fini M, Roffi A, et al. Regenerative Features of Adipose Tissue for Osteoarthritis Treatment in a Rabbit Model: Enzymatic Digestion Versus Mechanical Disruption. Int J Mol Sci. 2019;20:2636. doi: 10.3390/ijms20112636.
23. Lv X, He J, Zhang X, Luo X, He N, Sun Z, et al. Comparative Efficacy of Autologous Stromal Vascular Fraction and Autologous Adipose-Derived Mesenchymal Stem Cells Combined With Hyaluronic Acid for the Treatment of Sheep Osteoarthritis. Cell Transplant. 2018;27:1111-1125. doi: 10.1177/0963689718773333.
24. Veronesi F, Berni M, Marchiori G, Cassiolas G, Muttini A, Barboni B, et al. Evaluation of cartilage biomechanics and knee joint microenvironment after different cell-based treatments in a sheep model of early osteoarthritis. Int Orthop. 2021;45:427-435. doi: 10.1007/s00264-020-04701-y.
25. Cao KX, Tang HNA, Tran MH. Advances in hyaluronic acid therapy for knee osteoarthritis: monotherapy and combination strategies: an evidenced based review. Orthop Rev (Pavia). 2026;18:155103. doi: 10.52965/001c.155103.
26. Migliore A, Procopio S. Effectiveness and utility of hyaluronic acid in osteoarthritis. Clin Cases Miner Bone Metab. 2015;12:31-33. doi: 10.11138/ccmbm/2015.12.1.031.
27. In Y, Choi KY, Kim MS. Clinical Efficacy and Safety of Two Cycles of Intra-Articular Injection of Porcine Atelocollagen Versus Hyaluronic Acid in Knee Osteoarthritis. Bioengineering (Basel). 2025;12:710. doi: 10.3390/bioengineering12070710.
28. Naraoka T, Ishibashi Y, Tsuda E, Yamamoto Y, Kusumi T, Toh S. Periodic knee injections of collagen tripeptide delay cartilage degeneration in rabbit experimental osteoarthritis. Arthritis Res Ther. 2013;15:R32. doi: 10.1186/ar4181.
29. Svolacchia L, Prisco C, Giuzio F, Svolacchia F. Adipose Autologous Micrograft and Its Derived Mesenchymal Stem Cells in a Bio Cross-Linked Hyaluronic Acid Scaffold for Correction Deep Wrinkles, Facial Depressions, Scars, Face Dermis and Its Regenerations: A Pilot Study and Cases Report. Medicina (Kaunas). 2022;58:1692. doi: 10.3390/medicina58111692.
30. Erdayandi GE, Yilmaz O, Kerimoglu G, Sahin E, Dogan SY. Can intra-articular daidzein injection reduce oxidative damage and early osteoarthritis in a rabbit temporomandibular joint model? BMC Oral Health. 2024;24:1193. doi: 10.1186/s12903-024-04990-4.
31. Mehak F, Shabbir MA, Saeed M, Israr B. Chondroprotective effect of pomegranate seed oil in papain-induced knee osteoarthritis through animal modeling. J Agric Food Res. 2025;21:101903. doi: 10.1016/j.jafr.2025.101903.
32. Bai B, Li Y. Danshen prevents articular cartilage degeneration via antioxidation in rabbits with osteoarthritis. Osteoarthritis Cartilage. 2016;24:514-20. doi: 10.1016/j.joca.2015.10.004.
33. Goranov NV. Serum markers of lipid peroxidation, antioxidant enzymatic defense, and collagen degradation in an experimental (Pond-Nuki) canine model of osteoarthritis. Vet Clin Pathol. 2007;36:192-195. doi: 10.1111/j.1939-165x.2007.tb00208.x.
34. Grigolo B, Roseti L, Fiorini M, Facchini A. Enhanced lipid peroxidation in synoviocytes from patients with osteoarthritis. J Rheumatol. 2003;30:345-347.

35. Martins E, Cuervo B, Velasco-Martínez MG, Colomer-Selva R, Descalzo-Navarro M, Mena-Moros B, et al. Targeted Intra-Articular PRGF Delivery Using Enzyme-Powered Nanobots for Chondral Lesions: A Prospective Experimental Study with Biomarker Evaluation in Rabbits (Oryctolagus cuniculus). Animals (Basel). 2026;16:2010. doi: 10.3390/ani16132010.
36. Buckwalter JA, Anderson DD, Brown TD, Tochigi Y, Martin JA. The Roles of Mechanical Stresses in the Pathogenesis of Osteoarthritis: Implications for Treatment of Joint Injuries. Cartilage. 2013;4:286-294. doi: 10.1177/1947603513495889.
37. Onoi Y, Matsumoto T, Anjiki K, Hayashi S, Nakano N, Kuroda Y, et al. Human uncultured adipose-derived stromal vascular fraction shows therapeutic potential against osteoarthritis in immunodeficient rats via direct effects of transplanted M2 macrophages. Stem Cell Res Ther. 2024;15:325. doi: 10.1186/s13287-024-03946-3.
38. Tudorachi NB, Totu EE, Fifere A, Ardeleanu V, Mocanu V, Mircea C, et al. The Implication of Reactive Oxygen Species and Antioxidants in Knee Osteoarthritis. Antioxidants (Basel). 2021;10:985. doi: 10.3390/antiox10060985.
39. Bouglé A, Rocheteau P, Hivelin M, Haroche A, Briand D, Tremolada C, et al. Micro-fragmented fat injection reduces sepsis-induced acute inflammatory response in a mouse model. Br J Anaesth. 2018;121:1249-1259. doi: 10.1016/j.bja.2018.03.032.